PERGAMON

International Journal of Heat and Mass Transfer 42 (1999) 3137–3146

International Journal of HEAT and MASS TRANSFER

Digital computer simulation of dropwise condensation from equilibrium droplet to detectable size

B.M. Burnside*, H.A. Hadi [1]

Mechanical and Chemical Engineering Department, Heriot–Watt University, Riccarton, Edinburgh EH14 4AS, UK

Received 22 July 1998; received in revised form 5 November 1998

Abstract

A computer simulation of dropwise condensation of steam on a 240×240 μm surface with 60,000 randomly spaced nucleation sites is described. The maximum drop radius achieved was 3.9 μm, 0.21 ms after the start of condensation. Uniform radii drop generations noticed by Rose and Glicksman (1973) had not developed completely by 0.21 ms, although predicted to do so. The characteristic profile on the drop size histogram predicted by Tanaka (1979) extends to drop sizes smaller than have been observed in experiments. A peak heat transfer coefficient of just over 2 MW/m^2K was obtained, about twice the value measured by Tanasawa et al. (1978) immediately after the condensing surface had been wiped.

1. Introduction

This paper aims to study the growth and coalescence of drops in dropwise condensation of steam and the build up of drop size distributed from nucleation to a maximum radius of about 4 μm. It has proved impossible to do this by direct observation [1–5]. The technique used is computer simulation using more realistically high site density, surface size and number of time steps which is possible due to the increase in capacity and speed of modern computers over that available when previous simulations of dropwise condensation were attempted two decades ago [6–8].

Semi-theoretical calculation of heat transfer coefficients in dropwise condensation has been successful in predicting measured values. LeFevre and Rose [9] and Rose [10–12] based their approach on postulating what is in effect a drop population which was verified by experiment. This was elaborated by Rose and Glicksman [13]. They noticed from film frames taken by Westwater and his colleagues [3,14–16] that distinct generations of drops occupied the surface at any one time. They determined that the average radius of succeeding generations were in the ratio $\gamma \approx 0.19{:}1$ and the area of the surface left vacant by any one generation $f \approx 55\%$ of that occupied by the succeeding one. Based on expressions for the interfacial, curvature and conduction heat transfer resistances of the drops as a function of radius, an expression was obtained for heat flux through a drop of radius r and wall undercooling ΔT_{s-w}, at a given pressure [11]. This was integrated over the drop distribution to determine the average heat flux density q_{av} and the heat transfer coefficient, α_{dwc}.

Tanaka [17,19] developed a time-dependent theory, based on conservation of drops and their volume, to account for the changes in drop size distribution on the path of departing drops. In his initial paper Tanaka ignored all but the conduction resistance to heat transfer and worked with a low initial drop den-

* Corresponding author.

[1] Presently at Mechanical Engineering Department, Brunel University, U.K.

0017-9310/99/$ - see front matter
PII: S0017-9310(98)00372-X

Nomenclature

A	area
C_i	constants in Eq. 5
f	fraction of area between drops of $(i-1)$th generation occupied by drops of ith generation
h_{fg}	latent heat
k	thermal conductivity
l	distance between drop centres
N	nucleation site density
$N(r)$	drop population in range r, $r+dr$
q	heat flux density
Q	heat flux
r	drop radius
R	specific gas constant
x, y	Cartesian coordinates
t	time
T	temperature
V	condensate volume
v	specific volume

Greek symbols

α	steamside heat transfer coefficient
γ	ratio of radii of successive drop generations; condensation coefficient
ν	kinematic viscosity
ρ	density
σ	surface tension

Subscripts

av	average value
dwc	dropwise condensation
e	equilibrium value
f	liquid
growth	growth only, no coalescence
i	interfacial, initial
m, max	maximum, departure
min	minimum
O	initial
s	saturation
w	wall

sity of $10^6/cm^2$. Later [19] he included the effect of these resistances, increased the initial drop number and reduced the initial drop size to $2.1 \times r_e$. Plotted in log/log coordinates $N(r)$ vs r at various times in the cycle showed a characteristic profile: a shallow minimum followed closely by a maximum. This feature moved to higher drop sizes as time progressed. The profile at smaller values of r was independent of time and $N(r)$ was proportional to $1/r^{2.68}$. This region Tanaka called the equilibrium region of small drops where a characteristic steady distribution of microscopic drops exists. Notably, this index of r is equal to the value found by LeFevre and Rose [9] to fit heat transfer data well. However, later work by Rose [10] showed that an index of 2.5 fitted the results better, but only marginally.

At higher values of r, the slope of the profile was approximately independent of time. Tanaka called this the universal distribution for large drop range. The picture which emerges is that the surface soon after commencement of condensation is a little less than 40% covered by the larger drops, all of nearly the same size. Subsequently, a steady distribution of microscopic drops develops between the larger ones. As time goes on, the number of these drops of given radius remains constant. However, the size of the

larger drops increases and their numbers decrease due to coalescence. The size range of the microscopic drops can therefore increase and hence the droplet coverage of the surface, but the distribution of microscopic drop sizes remains steady. The theory predicted that $\alpha_{dwc} \propto 1/r_m^{0.32}$, at atmospheric pressure, very close to Tanasawa's [18] fit to experiment, $\alpha_{dwc} \propto 1/r_m^{0.31}$. Tanaka [2] confirmed the existence of the characteristic profile by measurements of drop size distributions from enlarged microscope photographs of steam condensation at 1.0l*b*, $q = 11{,}330$ and 430 kW/m^2 K. He noted [17] that, if the instantaneous values predicted by his theory are time averaged, then the characteristic hump of his predicted profile disappears and the resulting drop distribution agrees closely, in the range which could be observed, with that measured in other investigations of steam condensing at atmospheric pressure [1,4].

To date, the attempts to simulate dropwise condensation by digital computer have been limited by computer capacity. This set an upper limit on nucleation site density, N, and a lower limit on drop size or the length of the time steps employed. Gose et al. [6] carried out a computer simulation on a 100×100 grid containing 200 randomly distribution nucleation sites. On this scale maximum drop size before departure was allowed to vary between 0.5 and 18.8. Assuming a departing drop radius range of 0.8–1.25 mm these figures correspond to the unrealistically low maximum and minimum site densities of 1.1×10^3 and 0.3/cm^2. Further, only 25 time steps were used in each case for drops to grow from equilibrium to departure size. Because of the multiple overlapping of drops ensuing, this must lead to an unrealistic drop distribution. In their own computer simulation, Tanasawa and Tachibana [7] were able to use values of N up to only 3.2×10^3 sites/cm^2 and starting radii of about 40 μm. This led to an order of magnitude lower α_{dwc} than obtained by reliable measurements.

In the most sophisticated simulation so far, Glicksman and Hunt [8] divided the dropwise condensing cycle into a number of stages, starting with values of N up to 10^8/cm^2, corresponding to 1000 sites on a surface of 33×33 μm. Taking interfacial, curvature and conduction resistances into account, the growth and coalescence of drops was followed in an undisclosed interval of time, stated to be short, until either a single drop covered more than 4.5%, or seven drops covered 20% of the area. The former corresponds to a largest drop diameter of 7.9 μm, so that edge effects must have been considerable. Because of the size of the steps, overlapping of drops had occurred when the area around a large drop was examined for coalescences and the resulting drop centred on the original site. This does not allow for previous coalescences of smaller drops nearby which may lead to a drop which is larger than the one considered initially. Thus the position and distribution of drops after predicted coalescences may be different from the actual behaviour. The area of the second stage of condensation was increased by a factor of 10. Drops were redistributed on the surface by a procedure which resulted in equal heat transfer coefficients in transition between the stages and condensation rate in the area between these drops equal to the average rate in the previous stage. This was repeated until the stage in which a drop first reached the departure size. Only the first stage is relevant to the present study since the redistribution of drops at the end of this stage destroyed the natural distribution on the surface.

So far, then, no simulation from nucleation to detectable size sufficiently detailed and with a high enough site density has been reported. It is desirable that this be done to link the developing drop distribution with observations [1,3,4,14,16] and with the drop size distributions which form the basis of successful methods of predicting heat transfer coefficients [9,13,19]. This paper is aimed at bridging this gap. A detailed computer simulation is carried out over 60,000 nucleation sites with 10^8 sites/cm^2 on an area of 240×240 μm. Time steps are chosen to be the intervals between successive coalescences anywhere on the surface and are automatically generated by the simulation. The maximum drop size reached is about 4 μm.

2. Simulation

A Fortran 77 program was written to carry out the simulation. It was run on a 16 Mb ram, 50 MHz, PC. The details of the simulation are recorded elsewhere [20]. The condensed fluid was water and the following assumptions were made:-

1. Initially, the condensing area simulated has just been swept free by a falling drop and all nucleation sites are occupied by drops of twice the equilibrium size.
2. All drops at subsequent times are centred on a nucleation site.
3. Heat transfer resistance is made up of interface, curvature and conduction terms. The steam is free of air and the condensing surface has very high thermal conductivity so that constriction resistance is negligible.
4. Condensation coefficient is assumed to be unity in Eq. 2.
5. Drops are hemispherical (contact angle = 90°).
6. Coalescences are instantaneous and there is no waiting time in producing drops of twice equilibrium size on fixed nucleation sites whose positions are chosen randomly and all of which remain active during the simulation.

7. Drops formed by coalescence are centred on the site of the largest coalescing drop.

Following LeFevre and Rose [9] the heat flux Q through a drop of radius r at saturation temperature T_s and wall subcooling ΔT_{s-w} is

$$Q = \frac{\Delta T_{s-w} - \dfrac{2T_s\sigma}{h_{fg}\rho_f r}}{\dfrac{1}{\alpha_i 2\pi r^2} + \dfrac{1}{4k_f\pi r}} \tag{1}$$

where interfacial heat transfer coefficient α_i is given by [1]

$$\alpha_i = \frac{2\gamma}{2-\gamma}\,\frac{1}{(2\pi R T_s)^{\frac{1}{2}}}\,\frac{h_{fg}^2}{v_g T_s} \tag{2}$$

and γ is the condensation coefficient. The initial drop size r_i is taken to be twice the equilibrium size, r_e,

$$r_e = \left(\frac{2T_s\sigma}{h_{fg}\rho_f}\right)\frac{1}{\Delta T_{s-w}} \tag{3}$$

in order to speed up the mainly growth-by-condensation process which occurs at the smallest sizes. The rate of growth of a hemispherical drop, radius r, subject to heat interaction, Q is given by

$$\frac{dr}{dt} = \frac{Q}{\pi r^2}\,\frac{1}{2\rho_f h_{fg}} \tag{4}$$

Eliminating Q between Eqs. 1 and 4, and integrating the resulting equation leads eventually to the implicit equation for drop growth in a given time interval [20]

$$t_2 - t_1 = \frac{C_4}{2C_1}(r_2^2 - r_1^2) + \left\{\frac{C_3}{C_1} + \frac{C_4 C_2}{C_1^2}\right\}(r_2 - r_1) + \left\{\frac{C_3 C_2}{C_1^2} + \frac{C_4 C_2^2}{C_1^3}\right\}\ln\frac{C_1 r_2 - C_2}{C_1 r_1 - C_2} \tag{5}$$

where

$$C_1 = \frac{\Delta T_{s-w}}{2\pi\rho_f h_{fg}},\ C_2 = \frac{T_s\sigma}{\pi\rho_f^2 h_{fg}^2},\ C_3 = \frac{1}{2\pi\alpha_i},\ C_4 = \frac{1}{4\pi k_f}$$

A compromise between the size of the area to be studied and the density of sites was necessary because of the maximum capacity of the computer to store arrays of drop radii and the positions of the nucleation sites. The condition modelled was T_s = 100°C and $\Delta T_{s-w} = 3$ K. This corresponds to $r_e = 0.017$ μm, Eq. 3. According to Rose [11], $N = 0.037/r_e^2$, so that $N \approx 10^{10}/\text{cm}^2$. At this nucleation site density, only a small area could be studied with consequently unacceptable edge effects. Eventually, 60,000 sites were chosen on an area of 240×240 μm, so that $N = 10^8/\text{cm}^2$. The coordinates x and y of all nucleation sites were determined using a random number generator routine. All parameters in the program, including these coordinates were declared as double precision variables. To assist the computation, the simulation area was divided into 100 equal square regions. Fig. 1 shows the numbers of nucleation sites in each region. Fig. 2 is the overall flow chart for the simulation. At time zero (i = 1), all 60,000 nucleation sites are occupied by drops of radius r_i.

91	92	93	94	95	96	97	98	99	100
606	**570**	**577**	**615**	**563**	**598**	**617**	**585**	**611**	**614**
81	82	83	84	85	86	87	88	89	90
577	**593**	**610**	**580**	**621**	**589**	**600**	**592**	**613**	**568**
71	72	73	74	75	76	77	78	79	80
596	**620**	**587**	**587**	**621**	**600**	**622**	**627**	**639**	**632**
61	62	63	64	65	66	67	68	69	70
601	**593**	**601**	**579**	**598**	**639**	**640**	**563**	**585**	**588**
51	52	53	54	55	56	57	58	59	60
575	**605**	**638**	**608**	**609**	**570**	**596**	**574**	**648**	**615**
41	42	43	44	45	46	47	48	49	50
631	**600**	**596**	**627**	**597**	**604**	**637**	**642**	**620**	**612**
31	32	33	34	35	36	37	38	39	40
589	**616**	**623**	**607**	**579**	**580**	**573**	**615**	**611**	**593**
21	22	23	24	25	26	27	28	29	30
583	**560**	**589**	**623**	**570**	**634**	**604**	**600**	**596**	**572**
11	12	13	14	15	16	17	18	19	20
540	**593**	**585**	**596**	**604**	**585**	**591**	**570**	**644**	**639**
1	2	3	4	5	6	7	8	9	10
542	**609**	**645**	**608**	**600**	**593**	**567**	**629**	**569**	**583**

→Y

→X

Fig. 1. Distribution of nucleation sites over simulated area divided into 100 regions.

The technique used at this stage and at all subsequent times is shown in Fig. 3. In this figure there are six adjacent nucleation sites. A time step is assumed and the growth of all drops is calculated using a Newton-Raphson iteration for r in Eq. 5, ITERATION 1, Fig. 2. The program identifies the biggest overlap, $(r_4 + r_2) - l_{2-4}$, between any two adjacent drops. In Fig. 3a these are drops r_2 and r_4. The two drops centred on the bottom two sites r_6 and r_5 do not overlap any of the others. Time steps are reversed automatically using another Newton–Raphson iteration, ITERATION 2, Fig. 2, to determine the time at which r_2 and r_4 first touch. The radius of the other drops is also recalculated, ITERATION 3. The situation then is as in Fig. 3b. Having coalesced, the resulting drop is located on the site of the largest of the two, r_4, Fig. 3c, or randomly placed on one or other of the sites if they had been of equal size. The

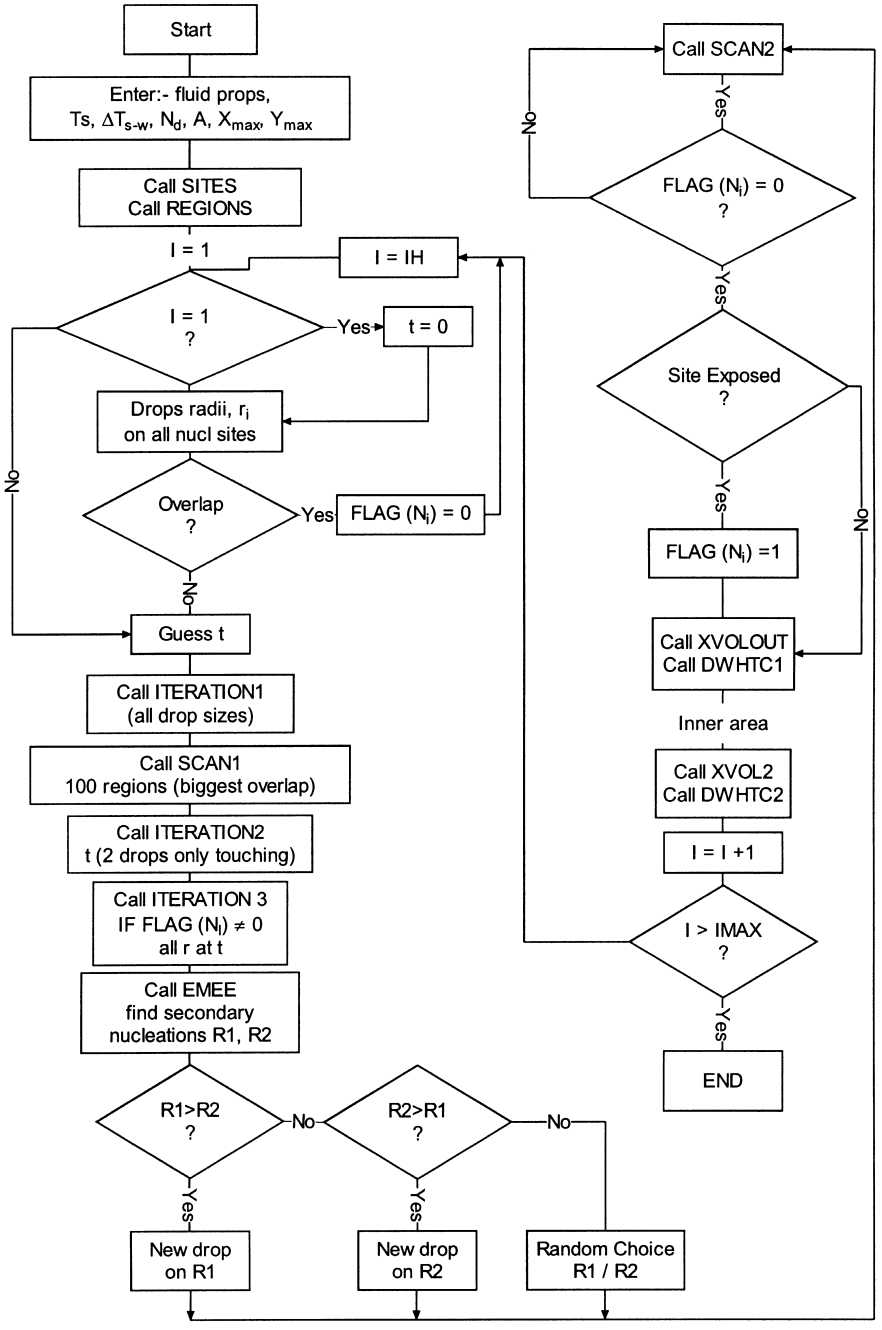

Fig. 2. Flow chart of main features of simulation program.

volume of the drop formed, V, is the sum of the volumes of the coalescing drops and its radius $r = \sqrt[3]{3V/2\pi}$. If the coalesced drop overlaps any of the adjacent drops, r_5 or r_6, as in Fig. 3c, coalescence is assumed to occur simultaneously with that of r_2 and r_4. The resulting situation is shown in Fig. 3d. It is possible that one of the coalescences may expose a nucleation site. For example, the final coalesced drop covers the adjacent nucleation site on which drops r_2 and r_6 were situated but not that on which r_5 was. On this site a drop of radius r_i is assumed to appear and to start to grow immediately. The same procedure was followed if any other nucleation sites, which were covered by any of the six original drops, were exposed by

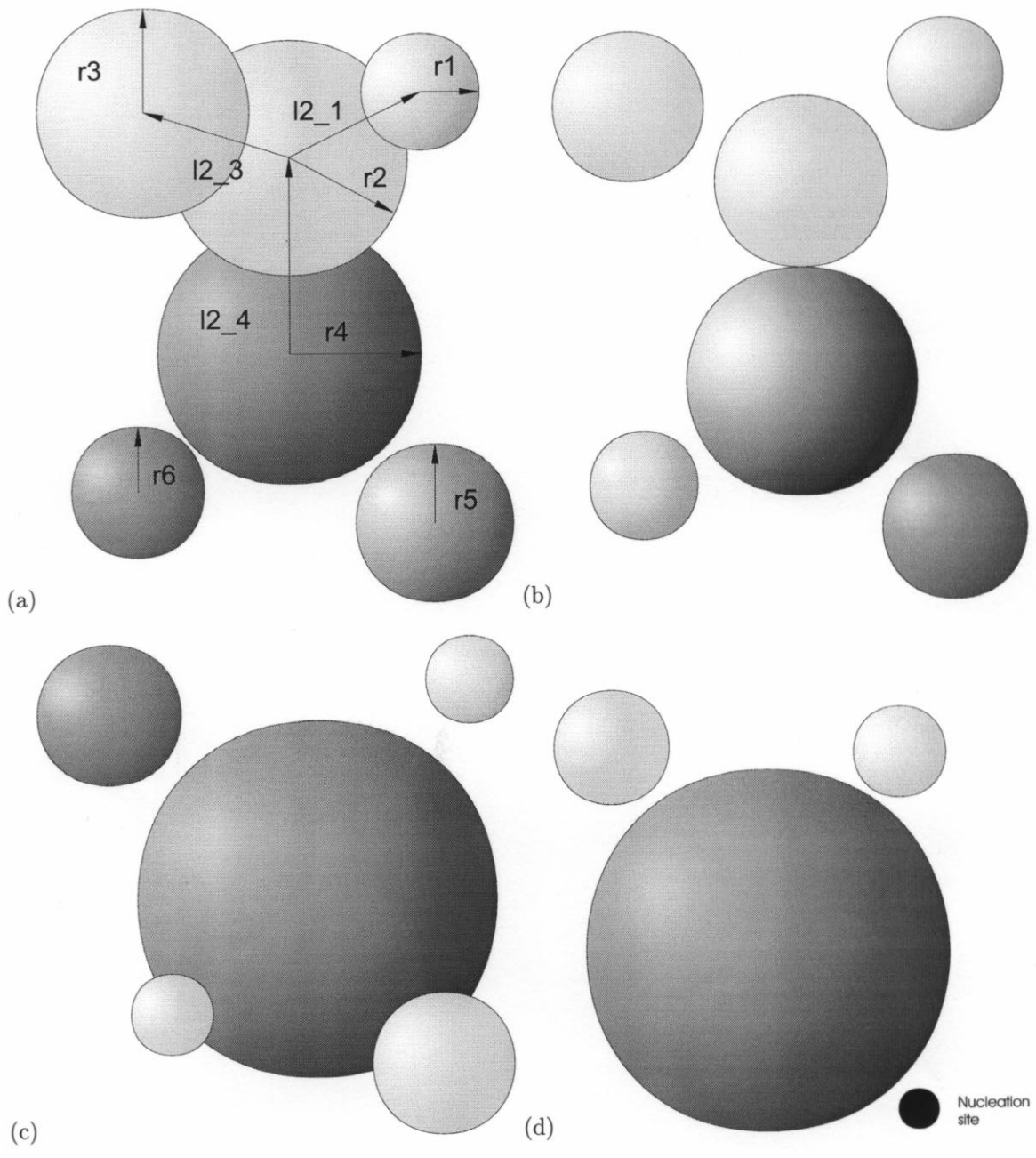

Fig. 3. Growth/coalescence simulation technique: (a) after initial time step $(r_4 + r_2) - l_{2-4} > (r_1 + r_2) - l_{2-1} > (r_2 + r_3) - l_{2-3}$: (b) after back stepping to point of initial coalescence: (c) coalesced drop sweeps up adjacent drops: (d) nucleation site is uncovered.

the coalescences. These covered sites, other than the ones on which the droplets were centred, were flagged at each time step and were revealed by a scan of the surface at subsequent times. The secondary coalescence procedure described above always resulted in all the liquid from the coalesced drops finding its way into the drop r_4, formed by the initial coalescence. Because of the additional time consuming screening which would have been involved, condition 7 above could not be observed during secondary nucleation.

After each time step and corresponding calculation of drop growth, the program first scans through the drops in all 100 regions, Fig. 1, to find the two drops which overlap the most. Then the technique described

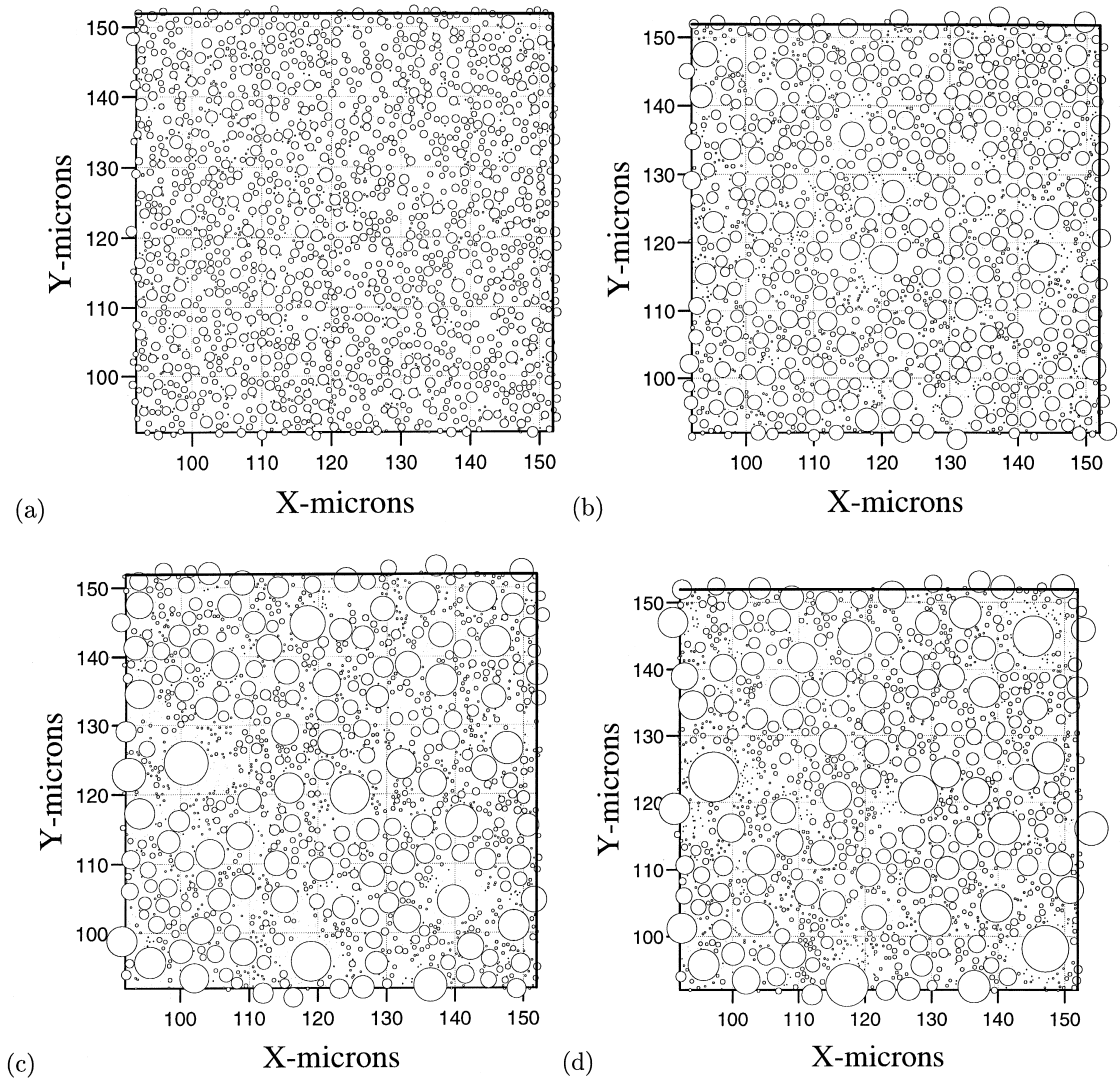

Fig. 4. Drop disposition over central part of simulated area during steam condensation cycle: (a) 0.07 ms: (b) 0.13 ms: (c) 0.19 ms: (d) 0.21 ms after sweeping by falling drop ($T_s = 100°C$, $\Delta T = 3$ K).

above is applied to a square = 20× the diameter of the largest of them. The process of identifying the two drops in question involves picking out each drop in turn and comparing its distance from all the others, with the sum of the radii. This is the most time-consuming part of the program and is speeded up considerably by making these comparisons only with drops in the same region, Fig. 1, or adjacent regions. A final scan of the whole surface is carried out to ensure that there are no further coalescences.

At each time step, the program calculates the volume of liquid inside the simulated area. This volume is not taken to include that part of any drops which overlap the boundaries of the simulated area, XVOLOUT, Fig. 2. Finally, the average heat transfer coefficient for the time interval, $\bar{\alpha}_{dwc}$ is calculated, DHWTC, Fig. 2

$$\bar{a}_{dwc} = \frac{\rho_f h_{fg}}{A\Delta T}\,\frac{\Delta V}{\Delta t} \tag{6}$$

where ΔV, A and Δt are the accumulated volume of condensate, the simulated area and the time step, respectively. As a check on edge effects $\bar{\alpha}_{dwc}$ is calculated, DWHTC2, Fig. 2, for an inner area, 200 × 200 μm in size, centred in the simulated area. Again, that part of the drops overlapping the boundary,

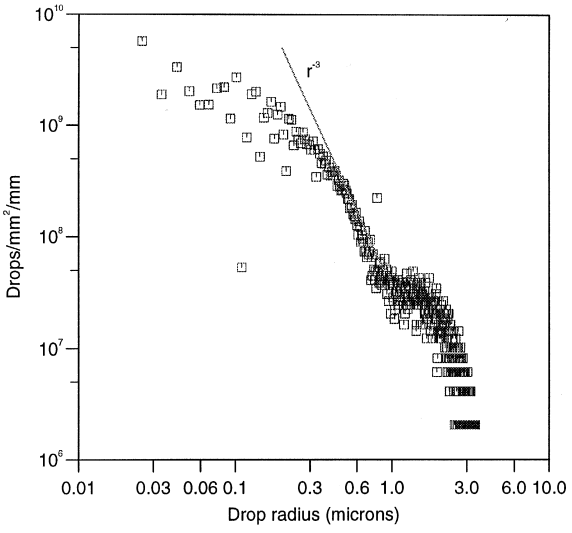

Fig. 5. Drop size distribution 0.21 ms after start of condensing cycle.

XVOL2, Fig. 2, is included in the calculation of the total condensate volume of the inner area.

3. Results and discussion

The simulation was run for 900 time steps, corresponding to 0.21 ms of the drop/coalescence cycle. Each of these time steps, which corresponded to the period between major coalescences, as described above, took 6–7 h of running time. The total number of coalescences which actually occurred was much greater than 900 because of the simultaneous coalescences which accompanied the ones ending the time steps. It was not possible to complete the simulation in one run due to the requirements of other users of the PC and because it was necessary to store the very large data files generated. At the end of the last run the largest drop radius was 3.5 μm. Fig. 4a–d show the development of the drops in the central 150×150 μm of the surface after time steps 260, 558, 792 and 901, corresponding to elapsed times of 0.07, 0.13, 0.19 and 0.21 ms from the start. These figures reveal the complexity of the process of drop development. In some cases the nucleation sites on which droplets have already coalesced with others of larger sizes, undergo many further nucleations before they are covered by the bigger coalesced drops. Also, once a drop centred on a nucleation site covers a neighbouring site, this site becomes inactive for a relatively long time until it is uncovered by coalescence of the drop covering it with a neighbouring larger drop. For that drop to attain this larger radius it must be far enough away to avoid

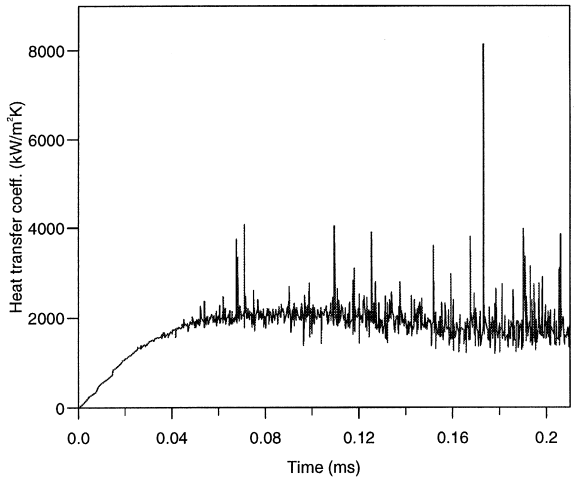

Fig. 6. $\bar{\alpha}_{dwc}$ vs. time based on outer area.

coalescing with the drop covering the original site before it exceeds its radius. Otherwise the site will remain inactive.

Fig. 5 is a histogram at 0.21 ms showing drop population as a function of radius. At each radius, r, the ordinate is the number of drops/mm in the radius range $r + 2.5r_e$ divided by the simulated condensing surface area in mm^2. Considerable scatter is noticeable especially at low drop sizes. This, particularly the very low point at just over 0.1 μm and the high point between 0.7 and 0.8 μm radius, is a consequence of the narrow radius range used in preparing the plot. Despite the scatter, it is evident that above about $r =$ 0.4 μm drop population, $N(r)$ has an inverse power law dependence on r with and index about 3 as shown in Fig. 5. Between 1 and 2 μm there is a point of

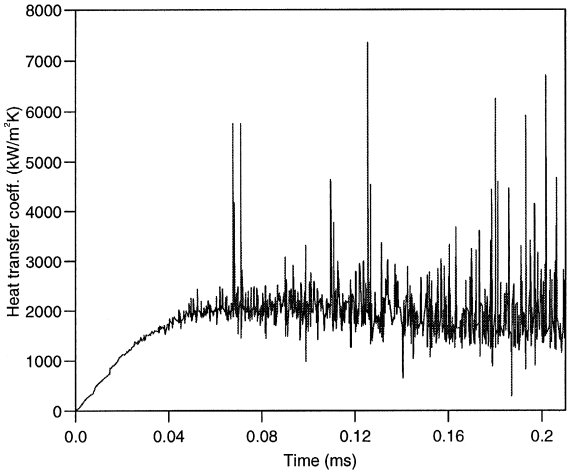

Fig. 7. $\bar{\alpha}_{dwc}$ vs. time based on inner area.

inflexion followed by a much steeper fall in drop population, which is similar to the behaviour predicted [17,19] and measured by Tanaka [2] at much higher drop radii, much further into the growth/coalescence cycle. The region of r^{-3} dependence of $N(r)$ is Tanaka's [2] equilibrium region of small drops. Fig. 5 is evidence that Tanaka's predictions extend to much lower radii than he was able to detect [2].

Figs. 6 and 7 show the heat transfer coefficients, $\bar{\alpha}_{dwc}$, Eq. 6, averaged over each time interval, calculated for the outer and inner areas. Scatter on these figures is caused by scatter in the values of the total volume of liquid, V, on the area in question at beginning and end of the time interval. Until about 40 μs drops are small and grow rapidly due to low conduction resistance. At this stage not many straddle the boundaries of the area. Later on there are more of these drops and they are larger. As they coalesce with larger neighbouring drops either inside or outside the boundary considered, there is a discrete change in the volume of liquid in the system. The result is a rapid fluctuation in liquid volume [20] and hence in heat transfer coefficient. Comparing Figs. 6 and 7, it is evident that the fluctuations in $\bar{\alpha}_{dwc}$ are generally less when referred to the outer area. This is because there are no nucleation sites outside the outer area, as there are outside the inner area, in the simulation as carried out. However, the agreement between the smoothed values of $\bar{\alpha}_{dwc}$ is an indication that edge effects do not invalidate the results of this investigation.

In both cases, Figs. 6 and 7, $\bar{\alpha}_{dwc}$ increases relatively smoothly up to 0.05 ms as the drops grow with few coalescences. After this it peaks to just over 2 MW/m^2 K at 0.09 ms before decreasing at the end of the simulation to about 1.7 MW/m^2 K. These values are very high compared to those obtained in practice where for most of the time the surface is covered by much larger drops over most of the growth/coalescence sweeping cycle. However, Tanasawa et al. [5] showed that rapid wiping of the condensing surface produced values of $\bar{\alpha}_{dwc} > 1\,\mathrm{MW/m^2\,K}$. They stated that they expected much higher values but could not measure them because of insufficiently fast response of the temperature measurements, incomplete sweeping by the wiper or a reduction in the expected numbers of active nucleation sites after the sweeping. The work reported here, although it extends only to 0.21 ms, shows a peak in $\bar{\alpha}_{dwc} > 2\,\mathrm{MW/m^2\,K}$ of only twice the value measured [5]. It should be mentioned that $\Delta T_{w-s} = 3$ K in the simulation compared to < 2 K initially in the measurements. Thus, the rate of growth of drops and hence $\bar{\alpha}_{dwc}$ is greater than in the experiments.

Fig. 8 shows the maximum drop radius as a function of time. Again, due to the randomness of drop coalescences, the rate of increase of r_{max} fluctuated with time. The figure shows the smoothed increase. Also

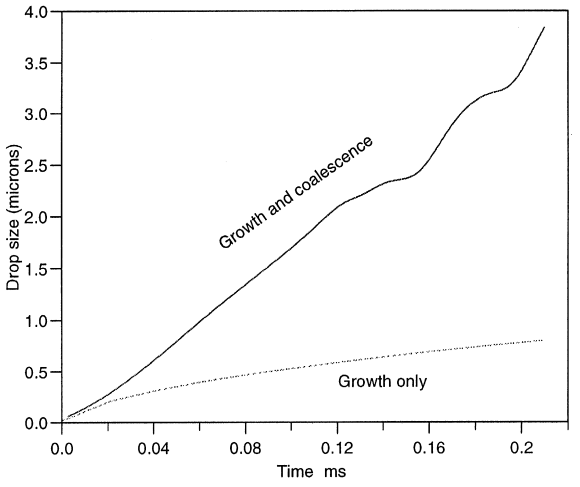

Fig. 8. Maximum droplet radius and isolated droplet radius vs. time.

plotted is the radius of drops which do not coalesce, r_{growth}. This was calculated by iterating in Eq. 5. The influence of coalescence even at this early stage in the condensing cycle is clear. At 0.21 ms a maximum drop four to five times that which would have occurred from growth alone is achieved.

Fig. 4 shows the development of the generations of drops noticed by Rose and Glicksman [13]. By 0.21 ms, Fig. 4d, these are still by no means distinct enough to calculate the ratio of succeeding generation sizes, γ, or the fractions, f, of the areas between each generation occupied by succeeding ones. The mean spacing between nucleation sites in the simulation is approximately ($240/60000^{0.5}$) μm or 1 μm. According to Rose and Glicksman [13] their drop generation model should be valid from when r_{growth} reaches half this mean spacing, i.e. 0.5 μm, or after 0.08 ms, according to Fig. 8, in this case. Examination of Fig. 3d, shows that even after 0.21 ms, when $r_{growth} = 0.8$ μm distinct generations had not developed completely. However, their computer simulation, starting with a random distribution of drop sizes, showed that the distinctness of drop generations on magnified microscope photographs of dropwise condensation, always developed. Thus the pattern shown at the end of the present simulation, Fig. 4d, must do the same, eventually.

4. Conclusions

A detailed simulation of dropwise condensation over an area 240×240 μm, nucleation site density, 10^8/cm^2, has been carried out, stopping when the maximum drop radius was about 4 μm. This covers the range it

is not possible to observe experimentally. This is the first simulation reported of this degree of sophistication and this size of surface with a realistic site density. The results can be compared to theoretical and semi-theoretical drop distributions which have been used as the starting point for successful time averaged calculations of heat transfer coefficients. The following are the principal conclusions:

1. The maximum drop radius reached by the growth/coalescence process was four to five times that reached by a growing drop which does not coalesce.
2. The gradual development of distinct drop generations, noticed by Rose and Glicksman [13] was evident but the absolute lower time limit at which their theory is valid should be set higher.
3. Tanaka's prediction [17,19] of a characteristic profile on the drop population vs drop size histogram and his equilibrium region of small drops where $N(r)\ \mathrm{d}r \propto r^{-3}$ is shown by this work to extend to drop sizes which are too small to have been observed in experiments.
4. A peak heat transfer coefficient of just over 2 MW/m^2 K was obtained which was about double the value measured by Tanasawa et al. [5] immediately after the condensing surface had been wiped.

Much faster personal computers have become available since the work was done. This offers the possibility of determining by simulation, the effect of changing nucleation site densities, steam conditions, contact angle and suppression of nucleation on sites uncovered by coalescences. Further, larger areas can be studied and the simulations run until generations visible in experiments can be seen and departure size reached, allowing time averaged heat transfer coefficients to be calculated for comparison with data.

Acknowledgements

The authors acknowledge the help of Mr Keith Miller in preparing the figures and thank the Department of Trade & Industry (U.K.) and National Power plc for studentship support (HAH).

References

[1] C.K. Graham, P. Griffith, Drop size distributions and heat transfer in dropwise condensation, International Journal of Heat and Mass Transfer 16 (1973) 337–345.
[2] H. Tanaka, Measurements of drop-size distributions during transient dropwise condensation, Journal of Heat Transfer 97 (1975) 341–346.
[3] J.F. Welch, J.W. Westwater, Microscopic study of dropwise condensation, in: Proceedings of the 2nd International Heat Transfer Conference, 1961, pp. 302–309.
[4] I. Tanasawa, J. Ochiai, Experimental study of dropwise condensation, Bulletin of the Japanese Society of Mechanical Engineers 16 (1973) 1184–1197.
[5] I. Tanasawa, J. Ochiai, Y. Funawatashi, Experimental study on dropwise condensation—effect of maximum drop size upon the heat transfer coefficient, in: Proceedings of the 6th International Heat Transfer Conference, 2, 1978, pp. 477–482.
[6] E.E. Gose, A.N. Mucciardi, E. Baer, Model for dropwise condensation on randomly distributed sites, International Journal of Heat and Mass Transfer 10 (1967) 15–22.
[7] I. Tanasawa, F. Tachibana, A synthesis of the total process of dropwise condensation using the method of computer simulation, in: Proceedings of the 4th International Heat Transfer Conference, 6 Cs1.3, 1970 pp.
[8] L.R. Glicksman, A.W. Hunt, Numerical simulation of dropwise condensation, International Journal of Heat and Mass Transfer 15 (1972) 2251–2268.
[9] E.J. LeFevre, J.W. Rose, A theory of heat transfer by dropwise condensation, in: Proceedings of the 3rd International Heat Transfer Conference, 2, 1966, pp. 362–375.
[10] J.W. Rose, On the mechanism of dropwise condensation, International Journal of Heat and Mass Transfer 10 (1967) 755–762.
[11] J.W. Rose, Further aspects of dropwise condensation theory, International Journal of Heat and Mass Transfer 19 (1976) 1363–1370.
[12] J.W. Rose, Condensation heat transfer theory, International Communications Heat Mass Transfer 15 (1988) 449–473.
[13] J.W. Rose, L.R. Glicksman, Dropwise condensation—the distribution of drop sizes, International Journal of Heat and Mass Transfer 16 (1973) 411–425.
[14] J.L. McCormick, J.W. Westwater, Nucleation sites for dropwise condensation, Chemical Engineering Science 20 (1965) 1021–1036.
[15] A.C. Peterson, J.W. Westwater, Dropwise condensation of ethylene glycol, Chemical Engineering Progress Symposium Series No. 64 62 (1966) 135–142.
[16] J.L. McCormick, J.W. Westwater, Drop dynamics and heat transfer during dropwise condensation of water vapour on a horizontal surface, Chemical Engineering Progress Symposium Series No. 64 62 (1966) 120–134.
[17] H. Tanaka, A theoretical study of dropwise condensation, Journal of Heat Transfer 97 (1979) 72–78.
[18] I. Tanawasa, J. Ochiai, Y. Utaka, S. En-ya, Experimental study on dropwise condensation—effect of departing drop size, Transactions of the Japan Society of Mechanical Engineers 42 (1976) 2846–2853.
[19] H. Tanaka, Further developments of dropwise condensation theory, Journal of Heat Transfer 101 (1979) 603–611.
[20] H.A. Hadi, Dropwise condensation: experimental and theoretical investigation. PhD thesis, Heriot–Watt University, Edinburgh, UK, 1996.